3D seismic imaging over two structurally complex surveys in the foothills of Pakistan

Rob Vestrum,[1*] Victor Dolgov,[1] Géza Wittman,[2] László Csontos[2] and Jon Gittins[1]

Abstract

In a tectonically complex area of northwest Pakistan, MOL Pakistan and its partners acquired two 3D seismic surveys. Extreme topography led to irregular shooting geometry. Varied surface access over this terrain required a mix of Vibroseis and dynamite source types to maximize subsurface coverage. With the combination of difficult surface conditions over a structurally complex subsurface, the data processing and merging of these two surveys required close attention to detail throughout the processing sequence, and we had to rely on the most robust algorithms in the data processing toolkit. There was no single technology that stood out in the processing, but by taking care at every stage in the processing sequence we were able to produce a readily interpretable seismic volume.

Introduction

The project area is on the Kohat Plateau of northern Pakistan. The geological setting of the exploration block is described in detail by Lorincz et al. (2008), Sercombe et al. (1998), and Wilson et al. (1993). The regional structures are three-dimensional in nature, resulting from transpressional forces in the collision zone between the Eurasia and India plates. In addition to compressional and transpressional tectonics, structures are influenced by the presence of ductile salt and clay diapir systems.

Figure 1 shows the project area in its regional tectonic setting. The region is at an area of convergence for three tectonic plates: the Indian Platform, the Afghan Block, and the Tibetan Block. Regional stresses include compressional and transpressional stresses as a result of these plate collisions. We felt that there were lessons learned in this project area that would translate to other tectonically complex settings.

MOL Pakistan contracted TBI to process and merge two 3D seismic surveys located in Exploration Block TAL in Khyber Pakhtunkhwa Province of Pakistan, previously known as the North-West Frontier Province. The main aim of the project was to get a more detailed structural image at the reservoir level. The problems to overcome in this project area included:

- Complex thrust tectonics
- Weathering and elevation corrections
- Shot-generated noise
- Irregular shooting geometry from rough terrain and surface conditions
- Merging of two oblique surveys with multiple source types

The problems listed above are typical in thrust-belt surveys. We took a toolbox approach to solving each problem as it arose, using a combination of recently developed technology and fundamental processes established by generations of trial-and-error in foothills exploration.

Prestack time migration (PSTM) from rough topography is an example of a robust, well established technology that overcomes difficulties resulting from complex thrust tectonics and rough topography, provided that velocities and statics are managed appropriately. In this example, new visualization technology for 3D PSTM velocity analysis proved to be extremely useful. In processing 3D seismic data from this tectonically complex area, no single technology stood out as the 'magic bullet' to improve the image, but careful attention to detail at all stages resulted in a readily interpretable seismic volume.

Geological setting

The structural geology map, shown in Figure 2, shows the surface expressions of the major structures over the TAL Block (Lorincz et al., 2008). Multiple episodes of deformation under different tectonic stress regimes have led to subsurface complexity and substantial variation in topographic relief. Exploration Block TAL is covered by Eocene to Pliocene sediments at outcrop, underlain by Mesozoic-Palaeocene sequences similar to those that crop out to the north. To the south, Palaeogene, Miocene, and Pliocene sediments have been thrusted over Pleistocene sediments along the Karak and Bandarbarra overthrusts. The Bannu Depression lies to the west and the Potwar Depression to the east. The southern parts of the Potwar Basin and the Kohat Plateau,

[1] *Thrust Belt Imaging, 2300 645 – 7th Ave SW, Calgary, Alberta T3H 4J9, Canada.*
[2] *MOL, Október Huszonharmadika u. 18., Budapest 1117, Hungary.*
* *Corresponding author, E-mail: rob@tbi.ca*

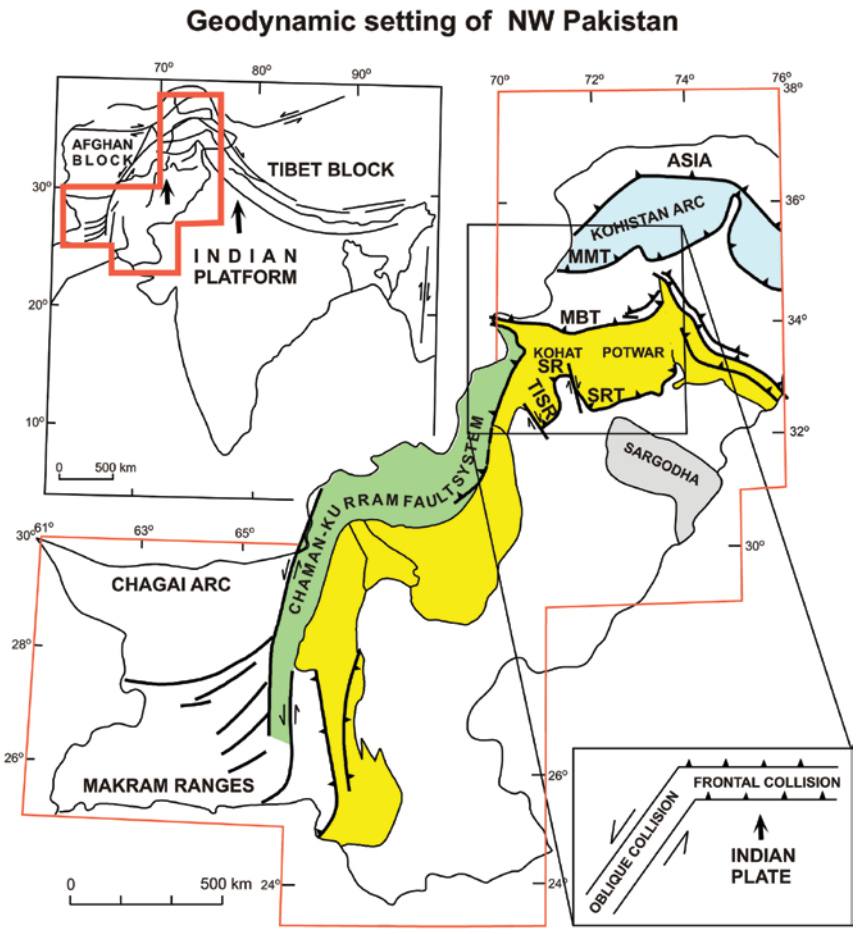

Figure 1 Location map showing regional tectonic setting of the project area.

including the Bannu Depression, are characterized by relatively flat-lying sediments, ranging in age from Palaeozoic to Pleistocene, with a northerly monoclinal dip (Figure 2).

As discussed by Abbasi and McElroy (1991), shortening in the Kohat Plateau was accommodated by at least two distinct detachment surfaces: the deep-seated Cambrian Salt and the shallower Palaeogene sequence. Seismic data and detailed field observations also suggest that the sedimentary sequence is divided into two units, separated by a regional detachment horizon that soles out at different stratigraphic levels depending on the lithology. In the north of the block, the detachment is within the lower part of the Eocene shales (Figure 3). In the southern part of the block, this detachment is within the younger Eocene section, which comprises thick evaporitic sequences including gypsum and halite.

The competent Palaeozoic and Mesozoic–Palaeocene sediments are folded in southward-verging asymmetric folds, the southern limbs of which are vertical or overturned. Although local, smaller structures may be present due to smaller internal detachments, the general shape of the folds is preserved throughout the sequence because the thick, competent formations give the backbone of the folds. At a smaller scale, the individual folds and thrusts can be interpreted as ramp anticlines forming a foreland-propagating stack. These imbricated folds are the main targets of exploration. The thrusts generally repeat a sequence of competent rocks that is about 1700 m thick. Tertiary foreland synclines of those anticlinal stacks are over-steepened, refolded by the late, out-of-sequence shortening. Folds and thrusts in the Tertiary sequence, above the Tertiary detachment, behave like passive roof backthrusts or detachment folds. Locally, E-W and NE-SW oriented shear zones may be super-posed on this imbricated structure. These shear zones typically form en echelon smaller fold sets and relaying faults.

The exploration team shot two seismic surveys over the southern part of the exploration block to image the subsurface targets. The blue outline on the geological map in Figure 2 shows the combined extent of the two surveys.

The 3D surveys

The two seismic surveys, Manzalai and Makori, were acquired with a mix of dynamite and Vibroseis, depending on surface access, so the two source types needed to be phase-matched before the surveys could be merged together. Table 1 lists the acquisition parameters for the two surveys. Fortunately, these were nearly identical in both surveys.

The shooting orientations of the two surveys are at an oblique angle to each other, with each survey following the orientation of the regional topography and the dominant

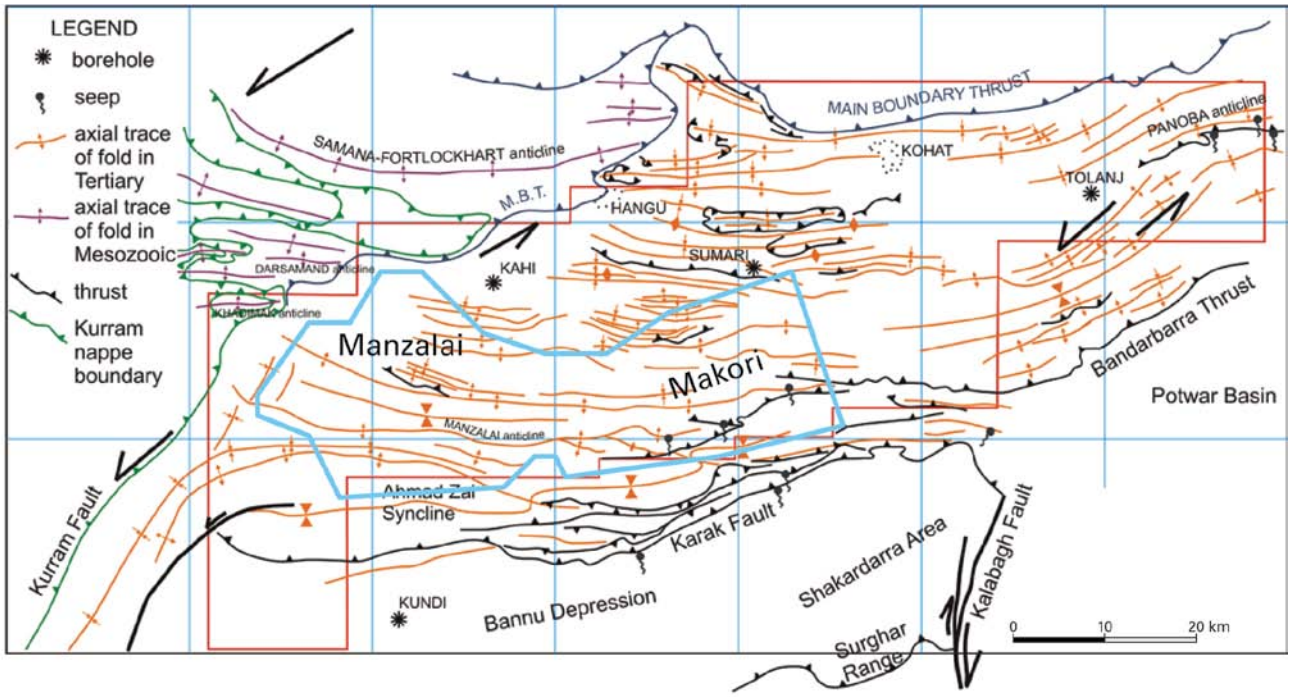

Figure 2 *Geological map of the surface structures over the TAL Block, outlined in red (after Lorincz et al., 2008). The blue polygon is the outline of the merged 3D seismic volume.*

subsurface dip direction. Figure 4a shows the source and receiver layout configuration for each survey. Note that throughout the surveys there are gaps in the source lines where surface conditions limited the surface access for source locations. Around the gaps, there is increased source effort to keep the fold of the subsurface coverage as high as possible. The overlap zone is where we matched the phase and statics between the merged surveys.

Figure 4b shows the elevation over the survey area. Note that the orientation of the topographic ridges varies across the survey area. The rough topography affected the positioning of the shot points (Figure 4a), and the variation in elevation of some 1000 m meant that we had to migrate these data from a rough topographic surface with strict quality control over our weathering statics.

Where the shooting geometry is spatially irregular and the elevation variation is large, Kirchhoff migration is the most robust seismic imaging algorithm in the processor's toolkit. It acts as a natural interpolator in irregular geometries and methods for Kirchhoff PSTM from surface topography are well established (e.g., Gray and Marfurt, 1995). The numerical efficiency of the algorithm combined with currently available computing technology allows us to run dozens of prestack migrations to be used in velocity analysis, as discussed in detail below.

Project objectives

Given the complexity in geological setting and resulting geophysical challenges, our inter-disciplinary team set the following objectives at the outset of the project:

	Manzalai	Makori
Shot line int	400 m	400 m
Shot interval	50 m	50 m
Traces per shot	1760 max	1920 max
Rec line int	400 m	400 m
Receiver interval	50 m	50 m
Nominal fold	55	55
Max offset inline	8750 m	9550 m
Max offset crossline	3600 m	3600 m
Shot depth	10 m	10 m
Geophone freq	10 Hz	10 Hz
String array	24 over 50 m	24 over 50 m
Source	Dynamite/ Vibroseis	Dynamite/ Vibroseis
Charge size	4 – 6 kg	4 – 6 kg
No. of vibrators	4	4
Sweep type	Linear	Linear
Sweep frequency	8 – 72 Hz	8 – 72 Hz
Sweep length	10 s	10 s

Table 1 *Acquisition parameters for the two surveys.*

- Merge oblique 3D surveys, each using both dynamite and Vibroseis
- Manage near surface complexity and rough topography
- Image steep-dipping reflectors and fault planes
- Use robust, tried-and-tested algorithms for difficult data with careful choice of processing parameters based on extensive testing

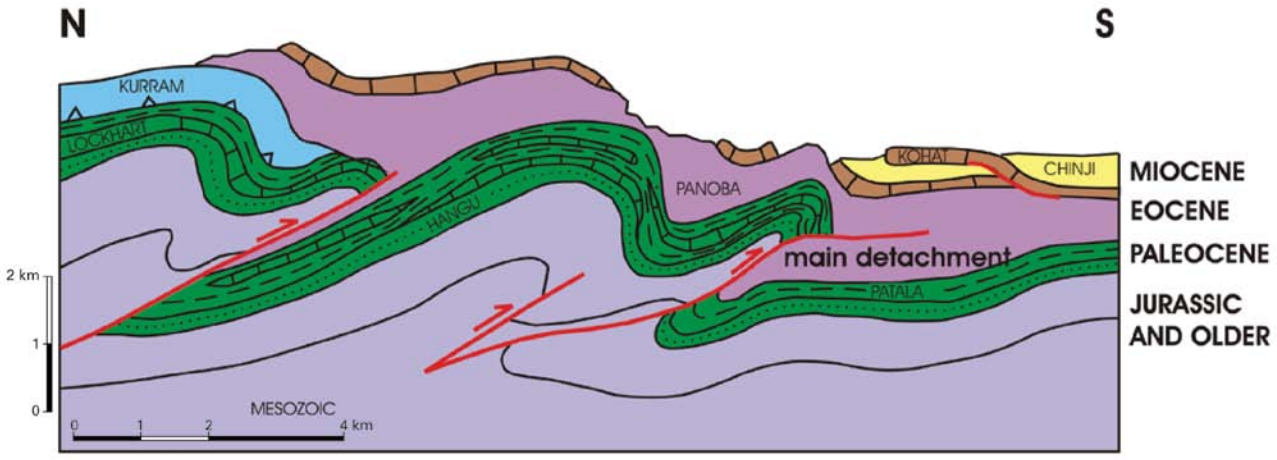

Figure 3 *Regional cross-section showing structural style over the block.*

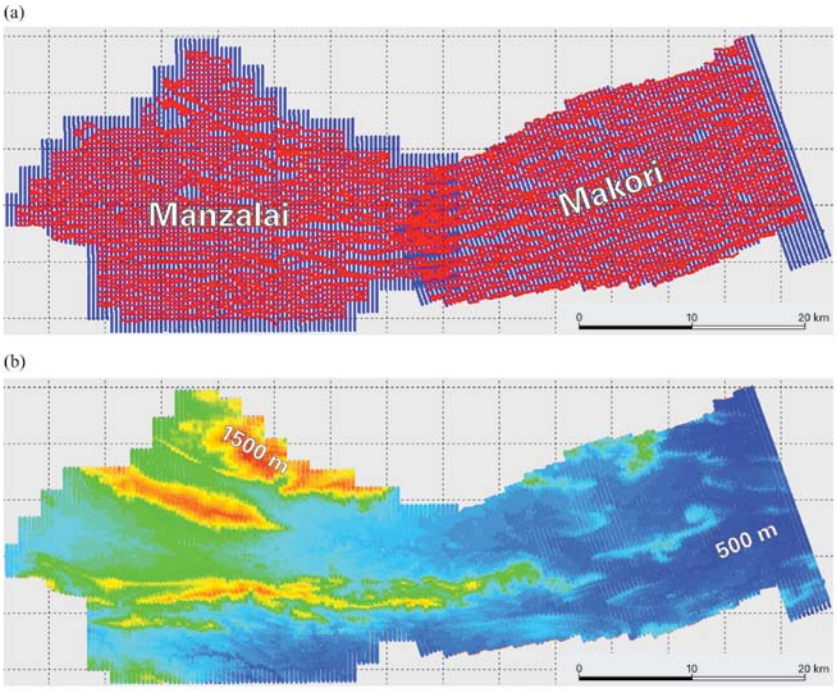

Figure 4 *(a) Shot and receiver map for both 3D surveys. Blue – receiver locations; red – source locations. (b) Elevation map. Elevation ranges from 500 m (blue) to 1500 m (red).*

The emphasis on robust algorithms was intended to compensate for the sensitivity of the seismic images to the choice of parameters, due to data irregularity, sparsity, and low signal-to-noise ratios. The back-to-basics approach to processing these data kept the workflow simple. Our plan was to direct the majority of our effort to managing statics and velocities, which are the two most sensitive parameters in imaging complex structures below rough topography.

Figure 5 shows the proposed workflow from our project plan. We followed this road map closely as the project progressed. Within each box of the workflow, we tested both alternative algorithms and parameters for each process. For example, in the refraction statics stage, we tested the three major refraction statics algorithms, first-arrival tomography, generalized linear inversion, and the layer-based time-term solution. We often find that the robust time-term solution results in a more stable statics solution and a more coherent stacked section, but in this case the first arrival tomography resulted in an improved stack image because it can more accurately handle rapid near surface velocity variation. The workflow box labelled MERGE (Figure 5) is the smallest box on the diagram, yet it represents one of the most crucial steps in resolving the imaging issues resulting from merging two surveys shot with different source types.

Merge of volumes and source types

The final volume had two separate volumes shot in different seasons, and each survey was shot with both dynamite and Vibroseis sources, depending on the surface-access conditions that vary throughout the area. Two surveys with two source

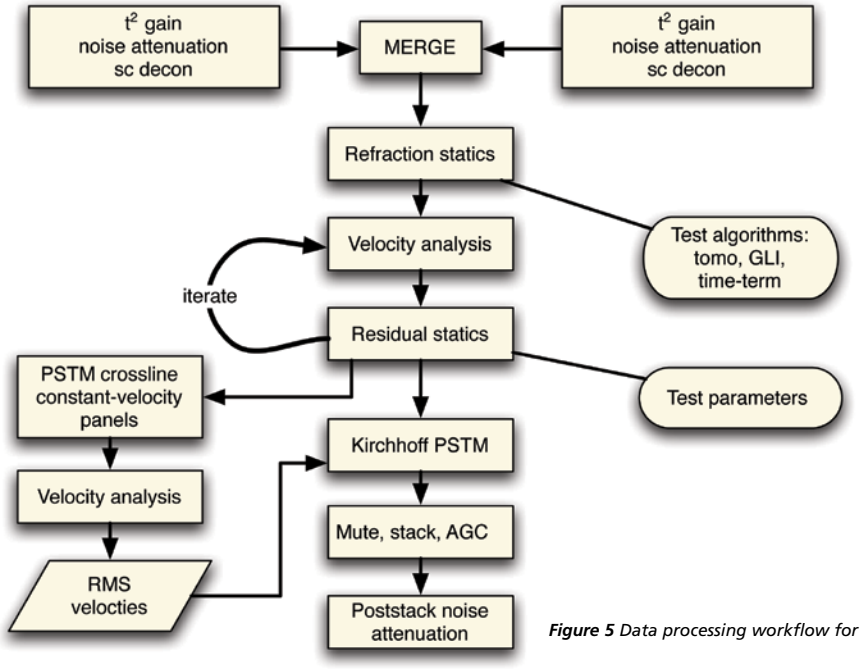

Figure 5 *Data processing workflow for merge of Manzalai and Makori 3D data volumes.*

types in each meant that we had to merge four data volumes, each with its own phase and amplitude characteristics.

To merge the two surveys, we used model-based wavelet processing, which is a technique for modelling the seismic wavelet in the processed data. The method, described by Connelly and Hart (1985) and again in more detail by Hart et al. (2001), models the phase and amplitude effects of the instrument and detector independently of the data. The model is then used to correct the seismic wavelet to zero phase. We derived and applied four independent filters, one for dynamite and one for Vibroseis for each of the two surveys.

Figure 6 shows before and after comparisons resulting from the application of model-based wavelet processing. At this stage of the processing, the diagnostic displays include inlines and crosslines from NMO stacked volumes. Before the application of model-based wavelet processing (Figure 6a), the stack shows reasonable reflectivity given the relatively noisy survey. The positions indicated by the arrows on Figure 6a and b show the transitional locations between Vibroseis and dynamite sources. It may be difficult to assess problems with mismatched phase in these zones judging by Figure 6a alone, but comparing the image to the same reflectors after model-based wavelet processing in Figure 6b, the improvement in coherency is readily apparent.

The more obvious improvement resulting from the wavelet processing is at the seam between the two surveys. The vertical black lines on Figure 6 indicate the location of the overlap zone between the two surveys. Before wavelet processing, there is a lack of coherency on most of the reflectors along this boundary (Figure 6a). After the merge, there is improved

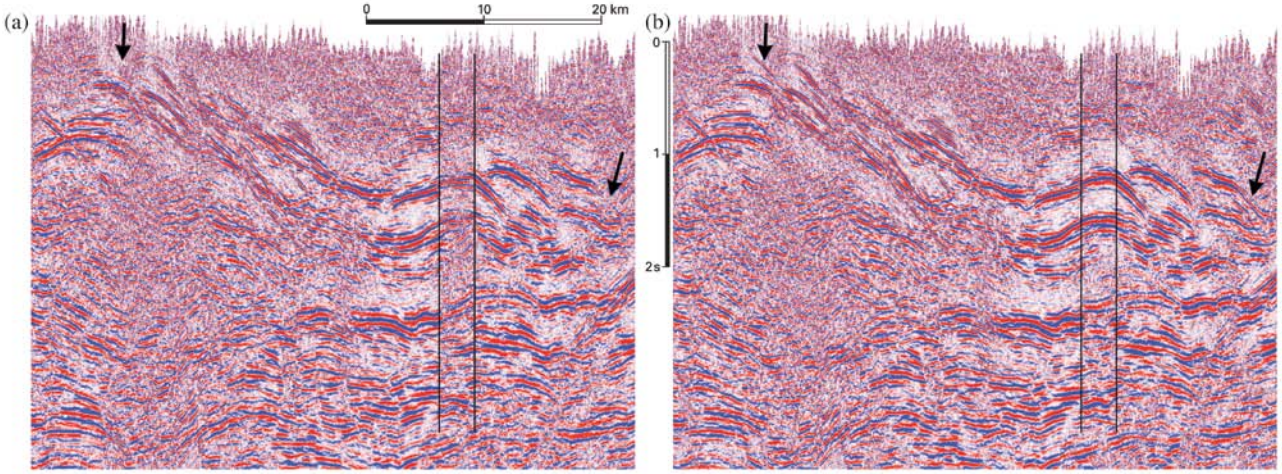

Figure 6 *NMO stack of part of a crossline from the merged volume (a) before and (b) after application of model-based wavelet processing. Arrows indicate locations where the wavelet processing matched Vibroseis and dynamite source signatures. Vertical lines indicate the overlap zone between the two surveys.*

coherency of events and consistent reflection character across the seam (Figure 6b). The image improvement resulting from matching source types is subtle compared to the coherency improvement at the boundary between the surveys.

Another consideration on the merge of the two volumes is the statics calculation. We calculated one refraction statics solution from the first breaks throughout the final seismic volume, over both surveys, accounting for both source types. The first breaks were picked considering the phase differences between dynamite and Vibroseis data. To ensure consistency of first break picking between the two source types, the processor first checked the pick times between adjacent dynamite and Vibroseis shots, and then inspected reflector continuity on the stack image across the source type transitions.

Once we had a phase match between the two source types over the two surveys and a refraction statics solution, we calculated residual statics over the entire survey. Figure 7 shows the comparison of an inline stack image, with normal moveout (NMO) corrections, before and after the application of residual statics. The most significant improvement to the image, marked by boxes in Figure 7, appears to be in the areas more dominated by dynamite or mixed dynamite/Vibroseis sources. As we had observed with the model-based wavelet processing, the improvement at the reflection statics stage is subtle, but with the low signal-to-noise ratio of these data, each incremental improvement was necessary to achieve an interpretable image.

Prestack time migration (PSTM)

Kirchhoff PSTM is the current workhorse of seismic imaging tools in land environments. Although new seismic imaging technologies continue to emerge, with great potential to reduce exploration risk in some environments, the stability and efficiency of the well established methods are highly desirable for foothills seismic imaging (Vestrum and Gittins, 2009). This quote from French (1990) continues to ring true 20 years later: 'In practical seismic imaging, we don't throw older technology away when new processes [are adopted].'

Kirchhoff migration is a summation process that is performed for input traces within a chosen aperture centred on the output point. For each input trace that contributes to each output sample, travel times are computed to determine the correct input sample to sum. No migration algorithm can compensate for gaps or low-density areas where the shooting did not adequately illuminate the subsurface structures, but the Kirchhoff summation process makes the algorithm less sensitive than other migration algorithms to irregularities in shooting geometry. On top of the irregularity caused by rough topography and surface-access issues, the natural grid Makori was at an oblique angle to the Manzalai grid, as shown in Figure 4a. The Kirchhoff algorithm migrated the data to the natural grid of the Manzalai 3D.

Finite difference or reverse time migrations are more sensitive to irregularity in acquisition geometry and the near surface complexity of an area like this makes regularization problematic. These and other high-fidelity algorithms are computationally intensive, and we relied on the short turnaround of Kirchhoff migration to run several iterations of constant-velocity migration for velocity analysis.

The computational efficiency of Kirchhoff migration coupled with the speed and low cost of currently available high performance computing technology offers the luxury of running many prestack migrations for analysis purposes. In this case, we migrated 70 constant-velocity PSTMs over a dense grid of velocity analysis lines. From this massive data volume, we used visualization tools to animate through the prestack-migrated stacked inlines and crosslines on the control grid and also to inspect the migrated image gathers for 'smiles' and 'frowns' that indicate which prestack migration velocity produces the flattest event (Zhu et al., 1998).

This velocity analysis methodology, described by Vestrum (2007), is illustrated by the screen captures from the velocity analysis program, VELANAL from Techco Geophysical (Figure 8). The method involves the inspection of migration-velocity effects in both offset and stack domains. This multi-domain analysis is important because PSTM

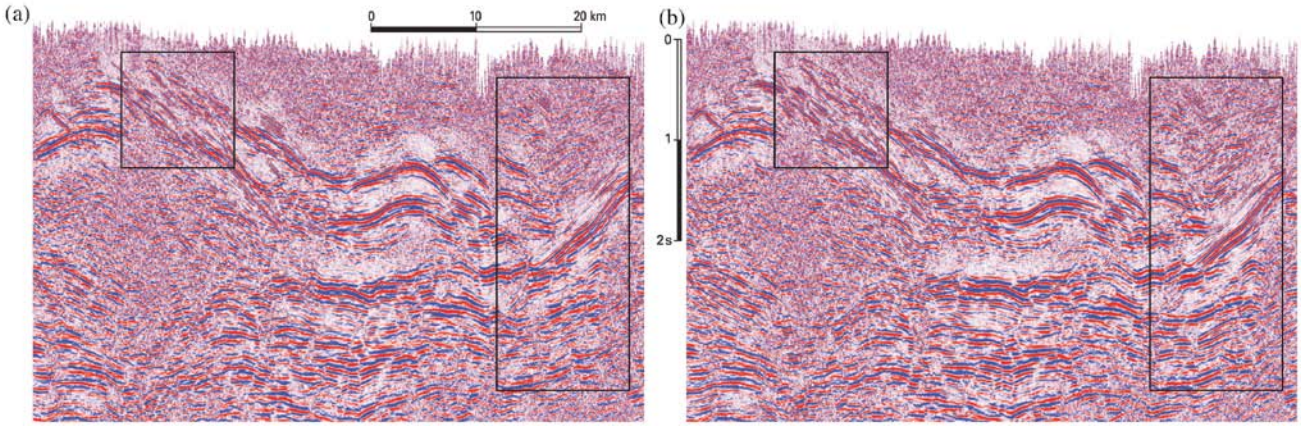

Figure 7 *NMO stack of part of a crossline from the merged volume (a) before and (b) after application of reflection statics. Boxes outline areas of improvement in reflector continuity.*

both corrects moveout in the offset domain and collapses diffractions in the stack domain. Limitations caused by assumptions inherent to time migration mean that the time migration velocity that most accurately corrects for offset may not be the same velocity that most accurately collapses diffraction energy. For an excellent discussion on why and how the seismic processing velocity differs from the true wave propagation velocity, see Al-Chalabi (1994).

This multi-domain analysis requires two types of input for each constant-velocity migration: a fully migrated section for each control line; and a migrated image gather for each velocity at the analysis points along every control line. The image-gather window (Figure 8a) shows a single common depth point (CDP) image gather migrated with 37 of the constant velocities. The location of the gather is indicated by the red arrow on Figure 8b. On CDPs with relatively high prestack signal-to-noise ratio, we used this display to quickly refine the velocity picks at a control point. In regions of low prestack signal-to-noise ratio, where the image gathers were ambiguous, or where the interpreter had concerns about the velocity sensitivity of the target reflectors, we went to the stack panel window (Figure 8b) and animated through all of the constant velocity panels to assess reflector coherency, migration operator noise, and the sharpness of reflector terminations. In the case of a velocity discrepancy, where the image gather was flat at one velocity and the stack showed a more geologically reasonable shape at another velocity, we chose the velocity that produced the better final image.

This analysis required seismic imaging experience and was done in collaboration with the interpretation team. The interpreters, in turn, learned about the velocity sensitivities of the imaged structures and gained understanding of the uncertainties involved in the seismic image. Throughout the velocity picking process, a composite stack of the input velocity panels (Figure 8c) closely simulates the PSTM that would result from the current velocity field for further quality control.

Processing after migration

In our quest to find imaging improvement at each step of the process, we tested various coherence enhancement and scaling techniques to the data after prestack migration of the full merged volume. What surprised us at this stage of

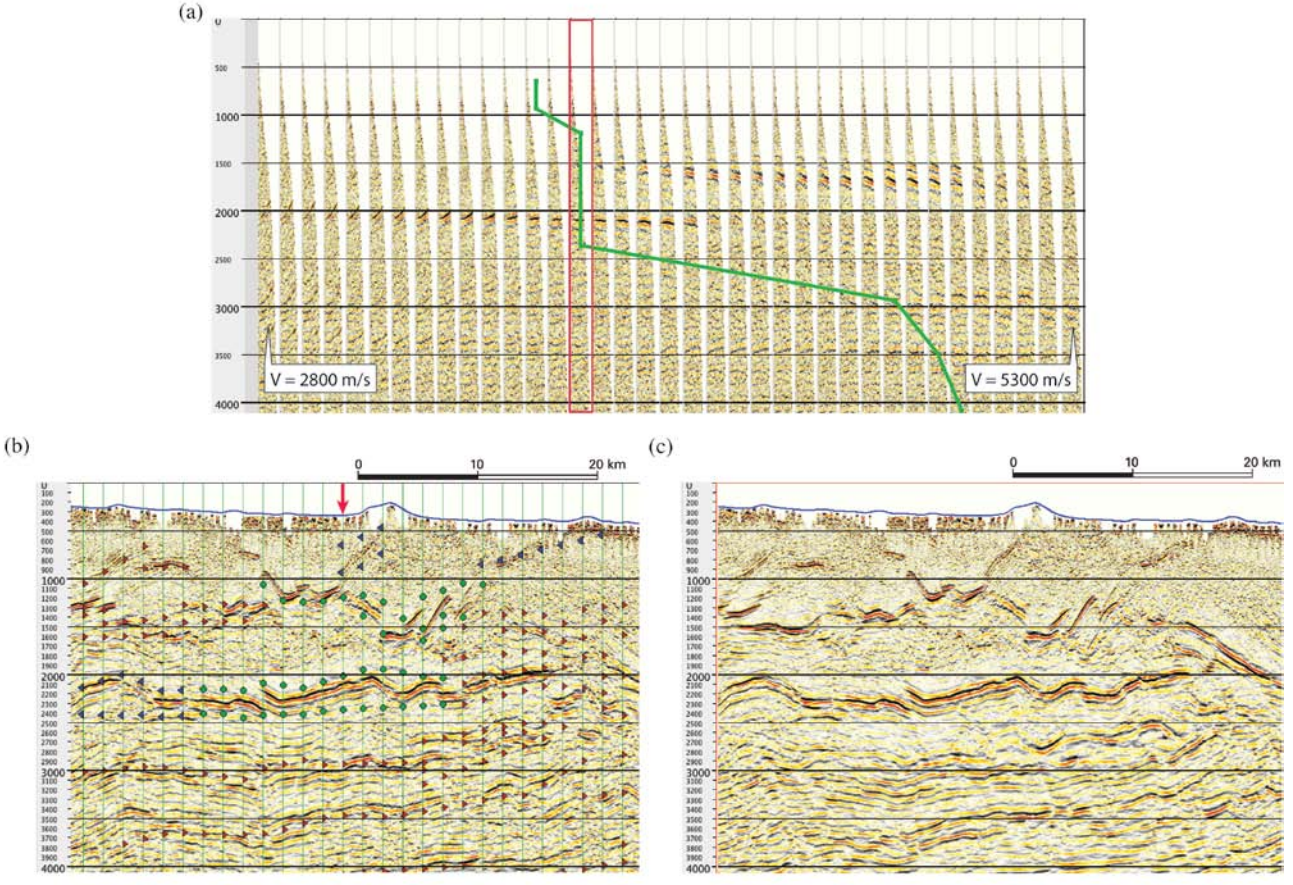

Figure 8 *Interactive velocity analysis for prestack time migration. (a) Image gather display showing migrated gathers over a range of velocites for the single CDP indicated by the red arrow in Figure 8b. Velocity picks are indicated by the green line. The red box indicates the 3800 m/s gather. (b) Stack panel display showing entire section at 3800 m/s migration velocity. The green dots are picks made on the current panel. Red and blue triangles indicate velocities picked higher and lower than the current panel, respectively. (c) Composite of the velocity stack panels given the current set of migration-velocity picks, which approximates the appearance of the final 3D prestack time migration.*

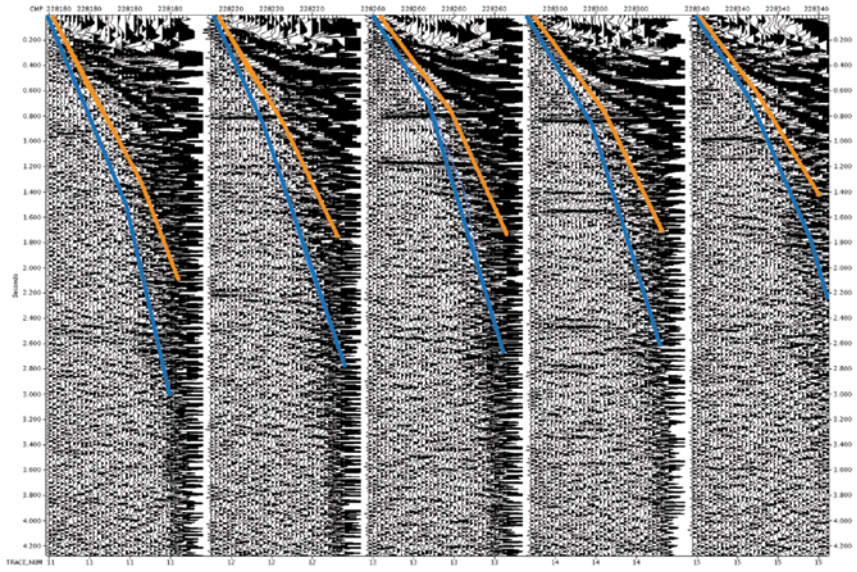

Figure 9 *Two mute functions picked on prestack-time-migrated image gathers.*

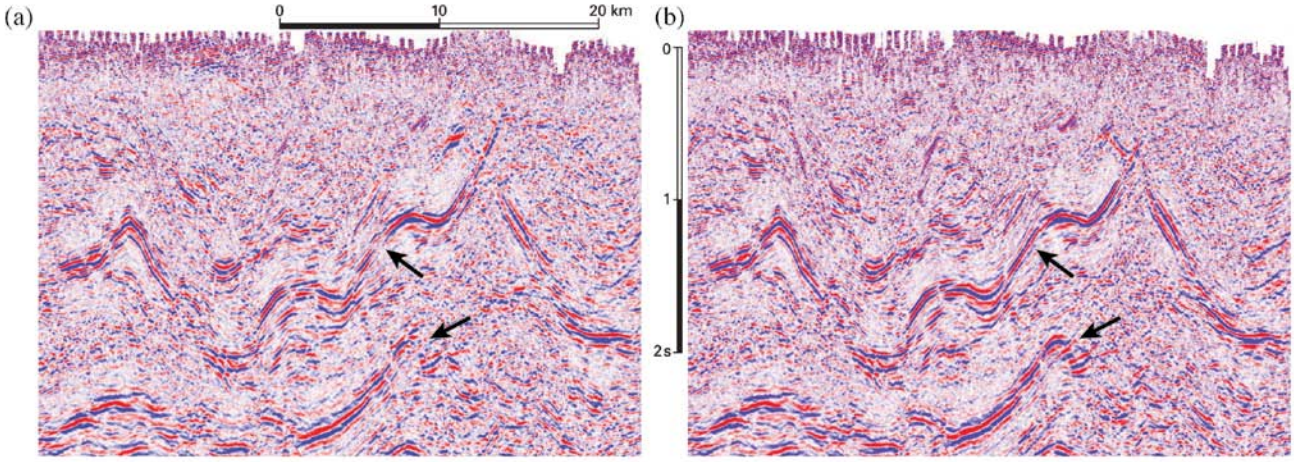

Figure 10 *Part of a crossline from the prestack-time-migrated stack with different mute functions applied: (a) mute picked to maximize noise removal, coloured blue in Figure 9; and (b) mute picked to maximize preservation of signal, picked orange in Figure 9. Arrows indicate reflectors with improved imaging.*

the processing was the large impact we observed with a small change in such a fundamental process as a prestack mute. Figure 9 shows two different mutes that we tested on the prestack migrated gathers. The blue mute was picked to ensure that all noise would be removed from the gathers before final stack. The orange mute was picked slightly more open in an attempt to capture more reflection energy. The results show a significant improvement in coherency of the steeply dipping reflectors with the application of the more open orange mute (Figure 10). Although mute is one of the most elementary processes applied to these data, refinement of the mute function made yet another subtle improvement to the coherency of the image.

Results and conclusions

The final imaged volume is shown in Figure 11. The irregularity in surface coverage is evident by the gaps in the near surface image. We were able to image reflectors throughout the seismic volume, and the image slices in Figure 11 show the significant complexity of deformation in this area. Steeply dipping reflectors are pervasive on both inline and crossline slices through the volume, illustrating the complexity of deformation in this transpressional geological setting.

Figure 12 shows the current PSTM volume as compared to the earlier processing. The cumulative effect of each incremental improvement in the seismic processing along the numerous steps in the processing flow is evident when comparing the current seismic image to the previous image. The comparison for crossline 500 (Figure 12a and b) shows subtle improvements throughout the section. Crossline 260 (Figure 12c and d) shows a more dramatic change in signal-to-noise ratio throughout the section. The cumulative effect of subtle imaging improvements at key steps along the workflow added up to a significant improvement in the interpretability of the image volume.

Seismic data processing and merging 3D seismic data volumes with multiple source types in this tectonically complex area required the most robust algorithms in the seismic

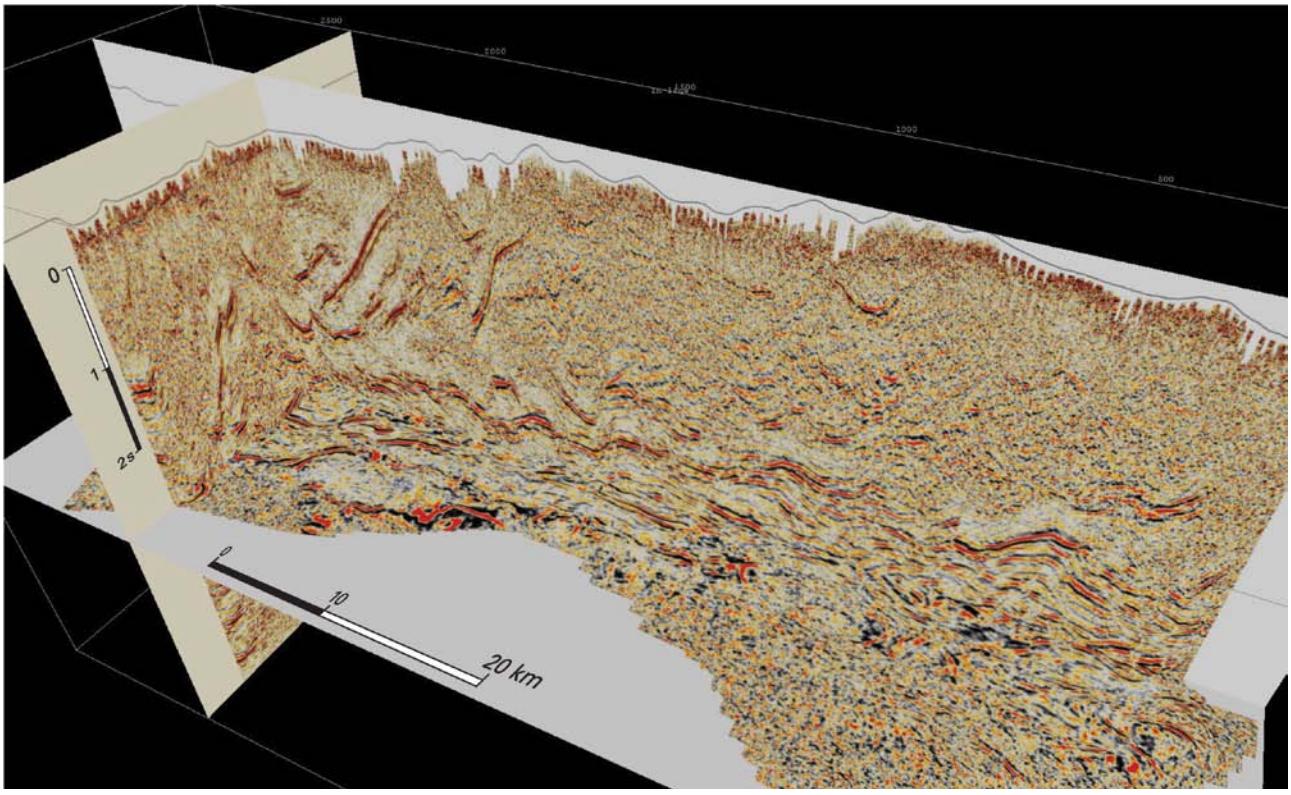

Figure 11 *Slices through the final prestack-time-migrated 3D volume showing structural complexity.*

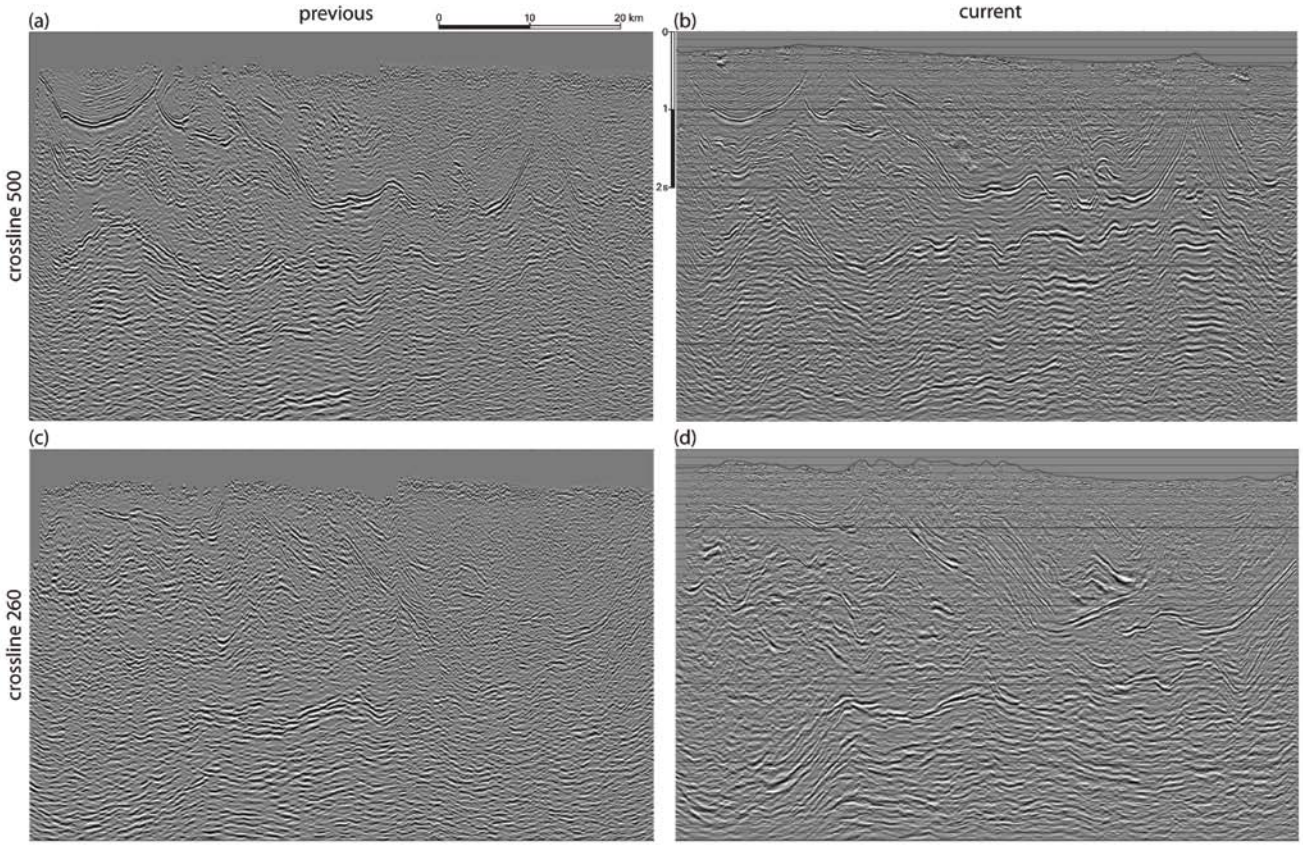

Figure 12 *Comparison between the previous and current versions of the seismic image for crosslines 500 and 260. (a) Previous image for crossline 500. (b) Current image for crossline 500. (c) Previous image for crossline 260. (d) Current image for crossline 260.*

toolkit to create an interpretable image volume. No single technology improved the image as much as careful attention to parameterization and quality control of the fundamental processes at each step along the workflow.

Acknowledgements

The authors thank MOL Pakistan and their exploration partners, Pakistan Petroleum, Government Holdings (Private), Pakistan Oilfields, and Oil and Gas Development Company, as well as Thrust Belt Imaging, for permission to publish this case history. We also appreciate the constructive comments of the reviewers.

References

Abbasi, I.A. and McElroy, R. [1991] Thrust kinematics in the Kohat Plateau, Trans Indus Range, Pakistan. *Journal of Structural Geology*, **13**, 319-327.

Al-Chalabi, M. [1994] Seismic velocities - a critique. *First Break*, **12**, 589-596.

Connelly, D. and Hart, D. [1985] Model-based wavelet processing of deconvolved seismic data. *SEG Annual Meeting*, Expanded Abstracts, **4**, 491-495.

Gray, S. and Marfurt, K. [1995] Migration from topography: improving the near-surface image. *Canadian Journal of Exploration Geophysics*, **31**, 18-24.

Hart, D.I., Hootman, B.W. and Jackson, A.R [2001] Modeling the seismic wavelet using model-based wavelet processing. *SEG Annual Meeting*, Expanded Abstracts, **20**, 1823-1826.

French, W. [1990] Practical seismic imaging. *The Leading Edge*, **9**(8), 13-20.

Lorincz, K., Ali, A., Csiki, I. and Csontos, L. [2008] Tectono-stratigraphic framework of TAL Block, Pakistan based on seismic interpretation. *70th EAGE Conference & Exhibition*, Extended Abstracts, P264.

Sercombe, W.J., Pivnik, D.A., Wilson, W.P., Albertin, M.L., Beck, R.A. and Stratton, M.A. [1998] Wrench faulting in the Northern Pakistan Foreland. *AAPG Bulletin*, **82**, 2003-2030.

Vestrum, R.W. and Gittins, J.M. [2009] Technologies from foothills seismic imaging: replacements or complements? *First Break*, **27**(2), 61-66.

Vestrum, R.W. [2007] Geoscience integration for seismic imaging in thrust-belt environments. *SEG Annual Meeting, Expanded Abstracts*, **26**, 2792-2796.

Wilson, W.P., Sercombe, W.J., Drowley, D.D., Van Nieuwenhuise, R.E., Albertin, M.L. and Stratton, M.A. [1993] Structure identification in a deformed belt – a wrench system in Pakistan. *55th EAEG Conference & Exhibition*, Extended Abstracts, A028.

Zhu, J., Lines, L. and Gray, S. [1998] Smiles and frowns in migration/velocity analysis. *Geophysics*, **63**(4), 1200-1209.

Received 2 October 2010; accepted 13 January 2011.
doi: 10.3997/1365-2397.2011013